

ARTICLE

 $F^2\Sigma^+-X^2\Sigma^+$ Band System of Cobalt Carbide

Jing-ru Guo, Zhao-xia Zhang, Ting-ting Wang, Cong-xiang Chen, Yang Chen*

Hefei National Laboratory for Physical Sciences at Microscale, Department of Chemical Physics, University of Science and Technology of China, Hefei 230026, China

(Dated: Received on May 30, 2008; Accepted on June 5, 2008)

The laser-induced fluorescence excitation spectrum of CoC was recorded in the spectral region from 13500 cm^{-1} to 22000 cm^{-1} , in which the CoC molecules were produced by the reaction of sputtered cobalt atoms with methanol under supersonic jet cooled conditions. Much of the visible spectrum was assigned to transitions between the $X^2\Sigma^+$ ground state and $F^2\Sigma^+$ state. The 11 bands assigned as ($v'=3-13, 0$) transitions of the $F^2\Sigma^+-X^2\Sigma^+$ band system were observed and rotationally analyzed. Equilibrium constants for the $F^2\Sigma^+$ state were $T_e=13628\text{ cm}^{-1}$, $\omega_e=669\text{ cm}^{-1}$, $\omega_e\chi_e=4.3\text{ cm}^{-1}$, $B_e=0.546\text{ cm}^{-1}$, and $R_e=1.758\text{ \AA}$. Some new bands were observed.

Key words: CoC, Laser-induced fluorescence, Spectrum

I. INTRODUCTION

The transition metal carbides have attracted much interest because of their importance in catalysis, biological processes, *ab initio* calculations, and organometallic chemistry. Among them, the 3d transition metal carbides are more important because some of them may be found in the circumstellar envelopes of carbon rich stars [1,2]. A large number of theoretical calculations on the 3d transition metal carbides have been reported on ScC [3], TiC [4-7], VC [8], CrC [9-11], FeC [12-16], CoC [17], NiC [18,19], and ZnC [20]. In contrast, experimental data of the spectra is available only for FeC [21-26], CoC [27,28], and NiC [29].

The first spectroscopy work on CoC was published in 1995 by Barnes *et al.* who reported the laser-induced fluorescence (LIF) study of CoC near 750 nm [27]. The ground state of CoC, $^2\Sigma^+$, was demonstrated to be an unusual Hund's case ($b_{\beta s}$) coupling. The low-lying $A^2\Delta$ state was observed in dispersed fluorescence. $A^2\Pi$ and an $\Omega=3/2$ excited states were also identified. Two bands at 13950 and 14635 cm^{-1} were assigned to be (0, 0) and (1, 0) of a $^2\Sigma^+-X^2\Sigma^+$ transition, respectively. At the same time, Adam and Peers observed ($v'=0-8, 0$) bands of this $F^2\Sigma^+$ (which was named [14.0] $^2\Sigma^+$)- $X^2\Sigma^+$ transition band system in low resolution spectra of CoC between 500 and 720 nm [28]. In their high resolution spectra, the (4, 0), (5, 0), and (7, 0) vibrational bands were analyzed. The $F^2\Sigma^+$ state was determined to be Hund's case ($b_{\beta j}$) coupling and originated from a $(8\sigma)^1(3\pi)^4(1\delta)^4(9\sigma)^2$ electronic configuration. Brewster and Ziurys carried out the millimeter wave study of CoC in 2001 [1]. Their results for the hyper-

fine structure of the ground state of CoC was in agreement with Ref.[27]. A very recent theoretical study on CoC reported spectroscopic constants and potential energy curves for seven lowest-lying doublet electronic states using multiconfigurational *SCF* and second-order perturbation theory [17]. This work suggested different energy order of the low-lying states. As for the $F^2\Sigma^+$ state, the spectroscopic constants were calculated to be $R_e=1.676\text{ \AA}$, $T_e=13342\text{ cm}^{-1}$, $\omega_e=1252\text{ cm}^{-1}$, and $D_e=3.17\text{ eV}$, in which the vibrational frequency 1252 cm^{-1} was two times larger than the experimental value [27,28].

The $F^2\Sigma^+-X^2\Sigma^+$ band system was observed as a long upper state vibrational progression with ($v'=0-8, 0$) transition bands in the $500-720\text{ nm}$ region [28]. In this work, we reinvestigated the $F^2\Sigma^+-X^2\Sigma^+$ band system of CoC in a wider spectral range. The LIF spectra in $460-730\text{ nm}$ revealed that this band system was much longer than expected. It was made up of 14 bands ($v'=0-13, 0$). The higher vibrational energy levels transitions were rotationally analyzed and more accurate equilibrium constants for the $F^2\Sigma^+$ state were obtained.

II. EXPERIMENTS

The gas-phase CoC molecules were produced by the reaction of sputtered cobalt atoms with methanol under discharge condition. Their spectra were recorded by LIF under supersonic jet-cooled conditions.

The experimental apparatus has been described in previous publications of our laboratory in detail [30,31] and will be outlined here briefly. About 2 kV voltage was supplied on a couple of cobalt electrodes for DC discharge. The sputtered cobalt atoms reacted with a pulse of saturated methanol vapor in argon carrier gas at a backing pressure of 606 kPa . The products expanded into the vacuum chamber, where the average working pressure was 40 mPa , and formed a super-

*Author to whom correspondence should be addressed. E-mail: yangchen@ustc.edu.cn, Tel.: +86-551-3606619, FAX: +86-551-3607084

sonic molecular beam. A pulsed dye laser (Lumonics: HD-500) pumped by a Nd:YAG laser (Spectra Physics: GCR-170) was used as the probe laser. The dye laser (with a linewidth of 0.1 cm^{-1} and a pulse width of 5 ns) crossed the molecular beam 3 cm downstream from the point of discharge. The excited fluorescence was collected by a set of lenses and finally recorded by a photomultiplier tube (Hamamatsu R928). The signal was amplified, averaged, integrated, and sent to the computer. The laser-induced fluorescence was collected orthogonal to both the molecular beam and the probe laser. The operation of the nozzle, the discharge, and the laser pulse were controlled sequentially by a multi-channel pulse generator. For lifetime measurements, the signal from the photomultiplier tube was digitized on an oscilloscope (Tektronics TDS 380) and the LIF decay curves were recorded by averaging the signals for 256 laser shots. The laser dyes used were LDS 698, DCM, Kiton Red 620, Rhodamine 590, Coumarin 540A, Coumarin 500, Coumarin 480, and Coumarin 460. All of them were products of Exciton Inc.. The laser wavelength was calibrated by optogalvanically active argon lines.

III. RESULTS AND DISCUSSION

Our first intention for employing the cobalt electrodes discharged in the presence of methanol gas was to produce CoH molecules. In the region $13500\text{--}18500 \text{ cm}^{-1}$, we found strong CoH signals. What made us even more excited was that CoC spectrum begins at 15800 cm^{-1} . A total of 11 bands assigned to the $(v'=3\text{--}13, 0)$ transitions of the $F^2\Sigma^+-X^2\Sigma^+$ band system were recorded. The intensities of the $F^2\Sigma^+-X^2\Sigma^+$ bands increase with vibrational quantum numbers of the upper states and reach a peak at $v'=9$, then gradually decrease. The (9, 0) band is so strong that the signal is saturated. The stick diagram in Fig.1 shows the relative intensities of all the observed bands.

Under our supersonic jet-cooled conditions, the rotational temperature is about 60 K. All the $F^2\Sigma^+-X^2\Sigma^+$ bands are red-degraded with the R branch forming a band head. There are so many rotational lines overlapped so that the R branch is completely unresolved. No Q branch is found. Every P branch is made up of two groups of rotational lines, and lines in every group are doubled. The magnitude of the intervals between the doubled lines is consistent with that of the G-splitting of the $X^2\Sigma^+$ ($v=0$) levels reported by Barnes *et al.* [27], which proved that these bands arose from the ground state. The $X^2\Sigma^+$ ground state of CoC is an unusual Hund's case ($b_{\beta s}$) coupling with large Fermi contact interaction. Only a few cases such as the ground state of ScO [32,33] and LaS [34] have been reported. The Hund's case ($b_{\beta s}$) coupling occurs when the Fermi contact interaction is much larger than the spin-rotation interaction. In this situation, the Fermi contact oper-

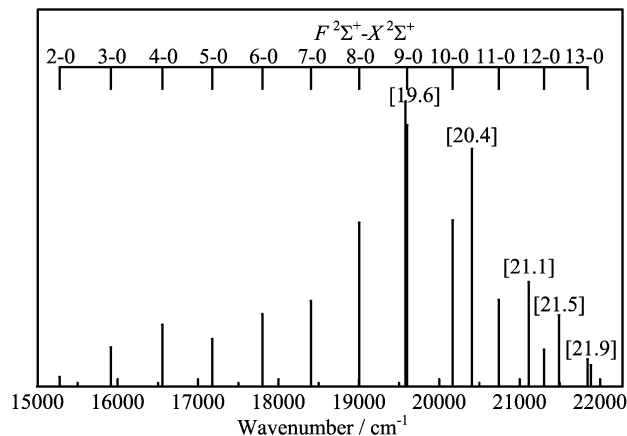


FIG. 1 The stick diagram of observed CoC bands against wavenumber. Approximate relative intensities of the bands are indicated by the height of the sticks.

ator, $b_F \mathbf{I} \cdot \mathbf{S}$, couples the vector \mathbf{S} to \mathbf{I} more strongly than the spin-rotation interaction couples \mathbf{S} to \mathbf{N} . The scheme of this coupling is

$$\mathbf{I} + \mathbf{S} = \mathbf{G}; \quad \mathbf{G} + \mathbf{N} = \mathbf{F} \quad (1)$$

The quantum number \mathbf{G} is the total spin. ^{59}Co has a nuclear spin $I=7/2$, and in the case of the $^2\Sigma^+$ state $S=1/2$, the rotational levels are split into $G=3$ and 4 components.

As stated by Barnes in Ref.[27], the rotational and hyperfine Hamiltonian for the $X^2\Sigma^+$ ground state consists of rotational, spin-rotational, hyperfine, and quadrupolar components.

$$H = H_{\text{rot}} + H_{\text{spin-rot}} + H_{\text{hf}} + H_{\text{quad}} \quad (2)$$

$$H_{\text{rot}} = BN^2 - DN^4 \quad (3)$$

$$H_{\text{spin-rot}} = \gamma \mathbf{N} \cdot \mathbf{S} \quad (4)$$

$$H_{\text{hf}} = b \mathbf{I} \cdot \mathbf{S} + c I_z S_z \quad (5)$$

$$H_{\text{quad}} = e T^2(\mathbf{Q}) \cdot T^2(\nabla E) \quad (6)$$

where B and D are the rotational constant and its centrifugal distortion respectively, γ is the spin-rotation parameter, b is the contact parameter, and c is the dipole interaction. The $c I_z S_z$ contribution to the energy is very small and can be neglected. Considering the low resolution of our spectra, influence of the nuclear electric quadrupole coupling also can be neglected. The rotational energy is $BN(N+1) - DN^2(N+1)^2$. The contact energies for $G=3$ and 4 are $-9/4b$ and $7/4b$, respectively. The spin-rotation energies are $-\gamma/16[F(F+1) - N(N+1) - 12]$ for $G=3$ and $\gamma/16[F(F+1) - N(N+1) - 20]$ for $G=4$. With F unresolved in our spectra, we take $F=N$ as approximation. Then the spin-rotation energies reduce to $3/4\gamma$ and $-5/4\gamma$ for $G=3$ and 4, respectively. The energy

TABLE I Molecular constants of $F^2\Sigma^+-X^2\Sigma^+$ transition of CoC (in unit of cm^{-1}).

Transition (v', v'')	T_v	B_v	$D_v \times 10^6$	γ	RMS	Lifetime/ μs
(3, 0)	15915.0	0.532(8)	0	0.112(4)	0.031	2.44(2)
(4, 0)	16553.9	0.528	6.9	-0.019		2.02(1)
	16553.57 ^a	0.5282 ^a	6.92 ^a	-0.0196 ^a		
(5, 0)	17176.4	0.526(5)	10.2	0.277(3)	0.021	1.19(2)
	17176.24 ^a	0.5251 ^a	47.4 ^a	0.2712 ^a		
(6, 0)	17799.2	0.524(6)	0	0.340(29)	0.025	1.39(2)
(7, 0)	18402.9	0.512(4)	0	0.253(25)	0.027	0.99
	18402.93 ^a	0.5128 ^a	0 ^a	0.2505 ^a		
(8, 0)	19003.1	0.516(5)	0	0.235(46)	0.054	0.68(4)
(9, 0)	19600					0.10
(10, 0)	20167.9(3)	0.507(19)	115	0.176(77)	0.12	0.64
(11, 0)	20741.3(2)	0.502(9)	16.2	0.142(56)	0.067	0.55
(12, 0)	21302.2	0.500	33.6	0.364(49)	0.056	0.44
(13, 0)	21844	0.49	0			0.70

^a Values in Ref.[28].

Error limits are 1σ , in units of the last significant figure quoted.

expressions for the $X^2\Sigma^+$ ground state are

$$E_3''(N) = T_v + BN(N+1) - DN^2(N+1)^2 - \frac{9}{4}b + \frac{3}{4}\gamma \quad (7)$$

(for $G=3$)

$$E_4''(N) = T_v + BN(N+1) - DN^2(N+1)^2 + \frac{7}{4}b - \frac{5}{4}\gamma \quad (8)$$

(for $G=4$)

The upper state of the $F^2\Sigma^+$ has been proved to be Hund's case (b_{β_s}) coupling with two spin-rotation components [28]. The energy level should be described as

$$E_1'(N) = T_v + BN(N+1) - DN^2(N+1)^2 + \frac{1}{2}\gamma N \quad (9)$$

$$E_2'(N) = T_v + BN(N+1) - DN^2(N+1)^2 - \frac{1}{2}\gamma(N+1) \quad (10)$$

$E_1'(N)$ and $E_2'(N)$ are for F_1 ($J=N+1/2$) and F_2 ($J=N-1/2$), respectively.

Spectroscopic constants were obtained by least squares fitting of every band to Eq.(7)-Eq.(10) provided perturbations by other states are insignificant. The constants for the ground state were fixed at the values in Ref.[27]. The results were listed in Table I. Since the R branches could not be resolved, only rotational lines of the four P branches were fitted. With about 30 lines in each band fitted, the RMS error 0.04 seems large. One of the main reasons is that we have just approximated the energy expression of the $X^2\Sigma^+$ ground state. The

spin-rotation terms were fixed as constants in Eq.(7) and Eq.(8), while the truth is that the contribution of the spin-rotation coupling to the energy increases with N [27]. That was also the reason for the very large error in γ value. The (0, 0) and (1, 0) bands at 13950 and 14635 cm^{-1} reported by Barnes *et al.* are too weak to be observed and the (2, 0) band appears only as a very weak band head at 15277 cm^{-1} . As for the most intense (9, 0) band, there is such serious overlap in the 19520-19610 cm^{-1} region that rotational lines of the (9, 0) band could not be distinguished.

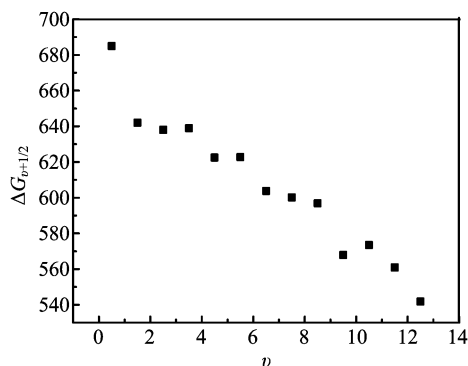
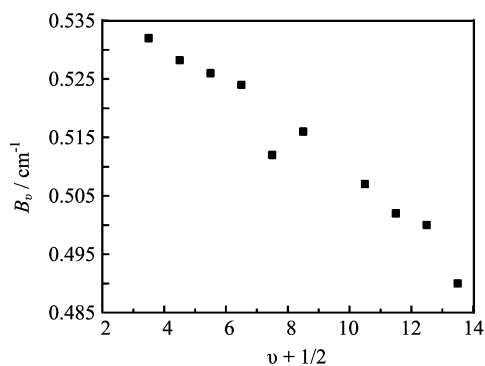
A fit of the band origins to the expression $T_v = T_e + \omega_e(v+1/2) - \omega_e\chi_e(v+1/2)^2$ gave the equilibrium constants of the $F^2\Sigma^+$ state, $T_e = 13628 \text{ cm}^{-1}$, $\omega_e = 669 \text{ cm}^{-1}$, and $\omega_e\chi_e = 4.3 \text{ cm}^{-1}$. The T_e value is a little larger than the theoretical 13175 cm^{-1} [17]. However, the ω_e value is only half of the calculated value [17]. $B_e = 0.546 \text{ cm}^{-1}$ was obtained by fitting the rotational constants (not including the B_v values of the $v'=7$ and 13 levels) to $B_v = B_e - \alpha_e(v+1/2)$. Also, the equilibrium bond length should be $R_e = 1.758 \text{ \AA}$.

Structures of the 3d transition metal diatomic are complicated because of widespread perturbations between many low-lying states. The vibrational levels of the $F^2\Sigma^+$ state spread over such a wide range of about 8000 cm^{-1} that perturbations seem unavoidable. Irregular variation of the vibrational intervals (together with the $v'=0$ and 1 levels in Ref.[27]) $\Delta G_{v+1/2}$ (Fig.2) and the rotational constants B_v (Fig.3) suggests complicated perturbation.

The lifetimes for these levels decrease rapidly from 2.44 μs (for $v'=3$) to 0.10 μs (for $v'=9$) (Fig.4) suggests strong mixing with short lifetime states nearby. The $v'=9$ level was the most seriously affected. Influence of the mixing upon the nearby $v'=8, 10$, and 11 levels

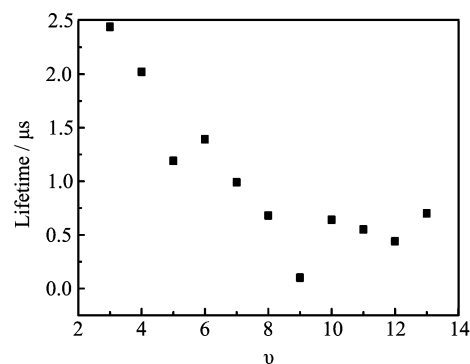
TABLE II Isolated band of CoC (in unit of cm^{-1}).

Band	T_v	B_v	$D_v \times 10^6$	γ	RMS	Lifetime/ μs
[19.6]						0.19
[20.4]						0.12
[21.1] (${}^2\Sigma^+-X^2\Sigma^+$)	21112.1	0.549(9)	21.1	0.333(4)	0.038	0.21
[21.5]						0.60(1)
[21.9] (${}^2\Sigma^+-X^2\Sigma^+$)	21885.4(1)	0.509(4)	0	0.181(3)	0.048	0.90(1)

FIG. 2 Vibrational intervals of the $F^2\Sigma^+$ state of CoC plotted as a function of v .FIG. 3 Rotational constants for the vibrational levels of the $F^2\Sigma^+$ state plotted as a function of $v+1/2$.

results in a large fitting error. The intrinsic lifetime for the $F^2\Sigma^+$ state was predicted to be longer than 2 μs . Strong bands with short lifetime upper states were observed at 19582, 20403, and 21112 cm^{-1} . These bands were labeled by energy in thousands of wavenumber as [19.6], [20.4], and [21.1]. The upper states of one or more of these bands are the possible candidates of the mixing states.

The $F^2\Sigma^+-X^2\Sigma^+$ band system is the strongest transition. We attempted to find all the bands reported in Ref.[27], but only the head of the 14071 cm^{-1} band can be observed. Transitions to the ${}^2\Pi$ upper state (which was $E^2\Pi$ in Ref.[17]) are too weak to be found. The experimental strength difference seems to be much greater than the calculation results, in which the os-

FIG. 4 Lifetimes for the vibrational levels of the $F^2\Sigma^+$ state plotted as a function of v .

cillator strength is $f=0.98 \times 10^{-3}$ for the $E^2\Pi-X^2\Sigma^+$ transition and $f=0.13 \times 10^{-2}$ for the $F^2\Sigma^+-X^2\Sigma^+$ transition.

The configuration for the $F^2\Sigma^+$ state was determined to be $(8\sigma)^1(3\pi)^4(1\delta)^4(9\sigma)^2$ [28]. It is a $8\sigma-9\sigma$ charge transfer promotion from the $(8\sigma)^2(3\pi)^4(1\delta)^4(9\sigma)^1$ configuration of the $X^2\Sigma^+$ ground state. This promotion is equivalent to moving an electron from a nonmetal-centered molecular orbital to a metal-centered one. The excitation usually causes a considerable increase in the bond length. The corresponding state arising from $8\sigma-9\sigma$ promotion for FeC is the $[13.17]^3\Delta$ state [23,25]. The bond lengths for both states are much larger than the corresponding ground state (in FeC, $R_e=1.754$ and 1.596 \AA for $[13.17]^3\Delta_3$ and $X^3\Delta_3$ state). Another common characteristic is the long lifetime. The $[13.17]^3\Delta_3$ state of FeC has lifetime about an order magnitude longer than the nearby $[13.1]^3\Phi_4$ state. In this work, the lifetimes for the less perturbed low vibrational levels for the $F^2\Sigma^+$ state of CoC are quite long. Although comparison with other states is not available, we did observe perturbation of short lifetime state.

Some other bands were observed. Two weak bands at 18670 and 19238 cm^{-1} were believed to rise from the $v''=1$ level of the ground state because they lie 931 cm^{-1} lower than the (9, 0) and (10, 0) band, respectively. Five isolated bands were observed, three strong bands, [19.6], [20.4], and [21.1], and two medium intensity bands, [21.5] and [21.9] (see Table II). The upper state of the [21.1] and [21.9] bands were Hund's case ($b_{\beta s}$) ${}^2\Sigma^+$ state, but it was not likely that these

two bands could be grouped together because of the large difference in rotational constants. In the spectra of RhC, there is a strong $E^2\Sigma^+-X^2\Sigma^+$ band system with short lifetime upper state [35,36]. The $E^2\Sigma^+$ state arises from the $(11\sigma)^2(4\pi)^4(2\delta)^4(12\sigma)^0(13\sigma)^1$ electronic configuration. We predict that the upper state of the [21.1] or [21.9] band may arise from the corresponding $(8\sigma)^2(3\pi)^4(1\delta)^4(10\sigma)^1$ configuration. The other three bands, [19.6], [20.4], and [21.5], are still under analysis. High resolution spectra and theoretical calculation on high lying states would be helpful.

IV. CONCLUSION

This work reinvestigated the LIF spectra of CoC in a wide range from 13500 cm^{-1} to 22000 cm^{-1} . Eleven bands of the $F^2\Sigma^+-X^2\Sigma^+$ band system were observed and rotationally analyzed. Irregular variation of the vibrational intervals and rotational constants indicated that the vibrational levels of the $F^2\Sigma^+$ were perturbed. The lifetimes change proved the mixing with some short lifetime states. Equilibrium constants for the $F^2\Sigma^+$ state of CoC obtained in this work were $T_e=13628\text{ cm}^{-1}$, $\omega_e=669\text{ cm}^{-1}$, $\omega_e\chi_e=4.3\text{ cm}^{-1}$, $B_e=0.546\text{ cm}^{-1}$, and $R_e=1.758\text{ \AA}$.

V. ACKNOWLEDGMENTS

This work was supported by the National Natural Science Foundation of China (No.20433080 and No.20673107), the National Key Basic Research Special Foundation of China (No.2007CB815203), and the Chinese Academy of Science (KJCX2-YW-N24).

- [1] M. A. Brewster and L. M. Ziurys, *Astrophys. J.* **559**, L163 (2001).
- [2] G. von Helden, A. G. Tielens, D. van Heijnsbergen, M. A. Duncan, S. Hony, L. B. Waters, and G. Meijer, *Science* **288**, 313 (2000).
- [3] A. Kalesos, A. Mavridis, and J. F. Harrison, *J. Phys. Chem. A* **105**, 755 (2001).
- [4] C. W. Bauschlicher Jr., and P. E. M. Siegbahn, *Chem. Phys. Lett.* **104**, 331 (1984).
- [5] M. D. Hack, R. G. A. R. Maclagan, G. E. Scuseria, and M. S. Gordon, *J. Chem. Phys.* **104**, 6628 (1996).
- [6] S. Sokolova and A. Luchow, *Chem. Phys. Lett.* **320**, 421 (2000).
- [7] A. Kalesos and A. Mavridis, *J. Phys. Chem. A* **106**, 3905 (2002).
- [8] S. M. Mattar, *J. Phys. Chem.* **97**, 3171 (1993).
- [9] I. Shim and K. A. Gingerich, *Int. J. Quantum Chem. Symp.* **23**, 409 (1989).
- [10] I. Shim and K. A. Gingerich, *Int. J. Quantum Chem.* **42**, 349 (1992).
- [11] R. G. A. R. Maclagan and G. E. Scuseria, *J. Chem. Phys.* **106**, 1491 (1997).
- [12] I. Shim and K. A. Gingerich, *Eur. Phys. J. D* **7**, 163 (1999).
- [13] S. S. Itono, T. Taketsugu, T. Hirano, and U. Nagashima, *J. Chem. Phys.* **115**, 11213 (2001).
- [14] D. Tzeli and A. Mavridis, *J. Chem. Phys.* **116**, 4901 (2002).
- [15] D. Tzeli and A. Mavridis, *J. Chem. Phys.* **118**, 4984 (2003).
- [16] D. Tzeli and A. Mavridis, *J. Chem. Phys.* **122**, 056101 (2005).
- [17] A. C. Borin, J. P. Gobbo, and B. O. Roos, *Chem. Phys. Lett.* **418**, 311 (2006).
- [18] I. Shim and K. A. Gingerich, *Chem. Phys. Lett.* **303**, 87 (1999).
- [19] A. C. Borin, L. G. M. de Macedo, *Chem. Phys. Lett.* **383**, 53 (2004).
- [20] A. Tsouloucha, I. S. K. Kerkines, and A. Mavridis, *J. Phys. Chem. A* **107**, 6062 (2003).
- [21] W. J. Balfour, J. Cao, C. V. V. Prasad, and C. X. Qian, *J. Chem. Phys.* **103**, 4046 (1995).
- [22] M. D. Allen, T. C. Pesch, and L. M. Ziurys, *Astrophys. J.* **472**, L57 (1996).
- [23] D. J. Brugh and M. D. Morse, *J. Chem. Phys.* **107**, 9772 (1997).
- [24] M. Fujitake, A. Toba, M. Mori, F. Miyazawa, N. Ohashi, K. Aiuchi, and K. Shibuya, *J. Mol. Spectrosc.* **208**, 253 (2001).
- [25] K. Aiuchi and K. Shibuya, *J. Mol. Spectrosc.* **209**, 92 (2001).
- [26] J. W. H. Leung, W. S. Tam, Q. Ran, and A. S. C. Cheung, *Chem. Phys. Lett.* **343**, 64 (2001).
- [27] M. Barnes, A. J. Merer, and G. F. Metha, *J. Chem. Phys.* **103**, 8360 (1995).
- [28] A. G. Adam, and J. R. D. Peers, *J. Mol. Spectrosc.* **181**, 24 (1997).
- [29] D. J. Brugh and M. D. Morse, *J. Chem. Phys.* **117**, 10703 (2002).
- [30] Y. Chen, J. Jin, C. J. Hu, X. L. Yang, X. X. Ma, and C. X. Chen, *J. Mol. Spectrosc.* **203**, 37 (2000).
- [31] J. Jin, Q. Ran, X. L. Yang, Y. Chen, and C. X. Chen, *J. Phys. Chem. A* **105**, 11177 (2001).
- [32] W. J. Childs and T. C. Steimle, *J. Chem. Phys.* **88**, 6168 (1988).
- [33] J. Shirley, C. Scurlock, and T. C. Steimle, *J. Chem. Phys.* **93**, 1568 (1990).
- [34] S. G. He, W. S. Tam, J. W. H. Leung, and A. S. C. Cheung, *J. Chem. Phys.* **117**, 5764 (2002).
- [35] H. Tan, M. Liao, and K. Balasubramanian, *Chem. Phys. Lett.* **280**, 423 (1997).
- [36] W. J. Balfour, S. G. Fougere, R. F. Heuff, C. X. W. Qian, and C. Zhou, *J. Mol. Spectrosc.* **198**, 393 (1999).